The metalloendopeptidase nardilysin (NRDc) is potently inhibited by heparin-binding epidermal growth factor-like growth factor (HB-EGF)

Véronique HOSPITAL*[1], Eiichiro NISHI†, Michael KLAGSBRUN†, Paul COHEN‡, Nabil G. SEIDAH* and Annik PRAT*[2]

*Laboratory of Biochemical Neuroendocrinology, Clinical Research Institute of Montreal, Montreal, Quebec H2W 1R7, Canada, †Departments of Surgical Research and Pathology, Children's Hospital and Harvard Medical School, Boston, MA 02115, U.S.A., and ‡Laboratoire de Biochimie des Signaux Régulateurs Cellulaires et Moléculaires, UMR 7631 CNRS, Université Pierre et Marie Curie, 96 Bd Raspail, 75006 Paris, France

Nardilysin (N-arginine dibasic convertase, or NRDc) is a cytosolic and cell-surface metalloendopeptidase that, *in vitro*, cleaves substrates upstream of Arg or Lys in basic pairs. NRDc differs from most of the other members of the M16 family of metalloendopeptidases by a 90 amino acid acidic domain (DAC) inserted close to its active site. At the cell surface, NRDc binds heparin-binding epidermal growth factor-like growth factor (HB-EGF) and enhances HB-EGF-induced cell migration. An active-site mutant of NRDc fulfills this function as well as wild-type NRDc, indicating that the enzyme activity is not required for this process. We now demonstrate that NRDc starts at Met^{49}. Furthermore, we show that HB-EGF not only binds to NRDc but also potently inhibits its enzymic activity. NRDc–HB-EGF interaction involves the 21 amino acid heparin-binding domain (P21) of the growth factor, the DAC of NRDc and most probably its active site. Only disulphide-bonded P21 dimers are inhibitory. We also show that Ca^{2+}, via the DAC, regulates both NRDc activity and HB-EGF binding. We conclude that the DAC is thus a key regulatory element for the two distinct functions that NRDc fulfills, i.e. as an HB-EGF modulator and a peptidase.

Key words: acidic domain, calcium binding, domain deletion, M16 family.

INTRODUCTION

N-arginine dibasic convertase (NRDc, or nardilysin; EC 3.4.24.61) was initially isolated as a putative proteolytic processing enzyme of precursors that transit through the secretory pathway [1,2]. *In vitro*, the endopeptidase cleaves dynorphin A (Arg ↓ Arg), α-neoendorphin (Lys ↓ Arg) and somatostatin-28 (↓ Arg-Lys) at basic sites and owes its acronym 'NRD' to its preference for cleaving at the N-terminus of Arg (R) residues in dibasic moieties [3,4]. Its subcellular localization [5,6], however, ruled out the possibility that the above *in vitro* substrates are cleaved *in vivo* by this enzyme. Indeed, while detected at the cell surface, the enzyme is mainly present in the cytosol and does not seem to enter the secretory pathway [6]. During mouse early development (embryonic day 10.5), high levels of NRDc transcripts are observed in the central nervous system and in cephalic and spinal ganglia. Expression then appears in many other tissues but remains dominant in the nervous and urogenital systems [7]. In the adult mouse, NRDc is particularly abundant in heart, skeletal muscle and testis [7–9]. In the latter tissue, NRDc accumulates in elongated spermatids where it is associated with the microtubular structure of the flagellum [5]. Paradoxically, it is also secreted by spermatids [5] and EL-4 thymoma cells [10]. The nature of its export mechanism remains to be elucidated.

NRDc presents an inverted consensus binding site, HXXEH, for catalytic Zn^{2+} and is thereby classified in the inverzincin/M16 family of metalloendopeptidases [11,12]. Insulysin [13,14], its closest mammalian homologue (32 % overall identity), shares 47 % identity in the ≈ 200 amino acid catalytic region conserved among the family members [15]. NRDc was the first reported M16 member to present an insertion in the catalytic region. This insertion is an acidic domain of NRDc (DAC), which in the rat sequence consists of a 71 amino acid acidic stretch (57 Glu + Asp) flanked by 12 N- and 7 C-terminal non-acidic residues [15]. While mouse NRDc exhibits an almost identical domain [16], the human one differs in that it has a shorter acidic stretch (53 amino acids; 43 Glu + Asp) [9]. Databank searches revealed the existence of six orthologues with insertions at exactly the same location (Figure 1): one each in *Arabidopsis thaliana* NRDc (AtNRDc) and zebrafish NRDc (zNRDc-SE), and two each in *Fugu rubribes* [Protein DataBank (PDB) codes Fr19825 and Fr29969] and *Drosophila melanogaster* (PDB codes dCG2025 and dCG10588). Like mammalian NRDc, AtNRDc and the two *Fugu* sequences show highly acidic insertions. On the other hand, those in zNRDc-SE and *Drosophila* orthologues are rich in Ser and Glu (SE insertions), plus Thr for dCG2025 (SET insertion). The latter insertions contain several potential phosphorylation sites that may contribute to the overall negative charge. In addition to its SET domain, dCG2025 also shows a 42 amino acid acidic stretch close to its C-terminus (Figure 1). It is intriguing that the alignment of NRDc with the other M16 family members starts at Met^{49} of rat NRDc (rNRDc). This suggests that rNRDc translation may not initiate at Met^{1}.

Very recently, NRDc was rediscovered at the cell surface of the breast cancer cells MDA-MB 453 as a binding protein for the heparin-binding epidermal growth factor (EGF)-like growth

Abbreviations used: NRDc, N-arginine dibasic convertase; DAC, acidic domain of NRDc; EGF, epidermal growth factor; EGFR, EGF receptor; GST, glutathione S-transferase; HB, heparin-binding; HB-EGF, heparin-binding EGF-like growth factor; MMP, mitochondrial processing peptidase; ORF, open reading frame; rNRDc, rat NRDc.

[1] Present address: Institut Pasteur, Laboratoire de Signalisation Immunoparasitaire, URA 1960 CNRS, Département de Parasitologie, 25 rue du Dr Roux, Paris, France.

[2] To whom correspondence should be addressed (e-mail prata@ircm.qc.ca).

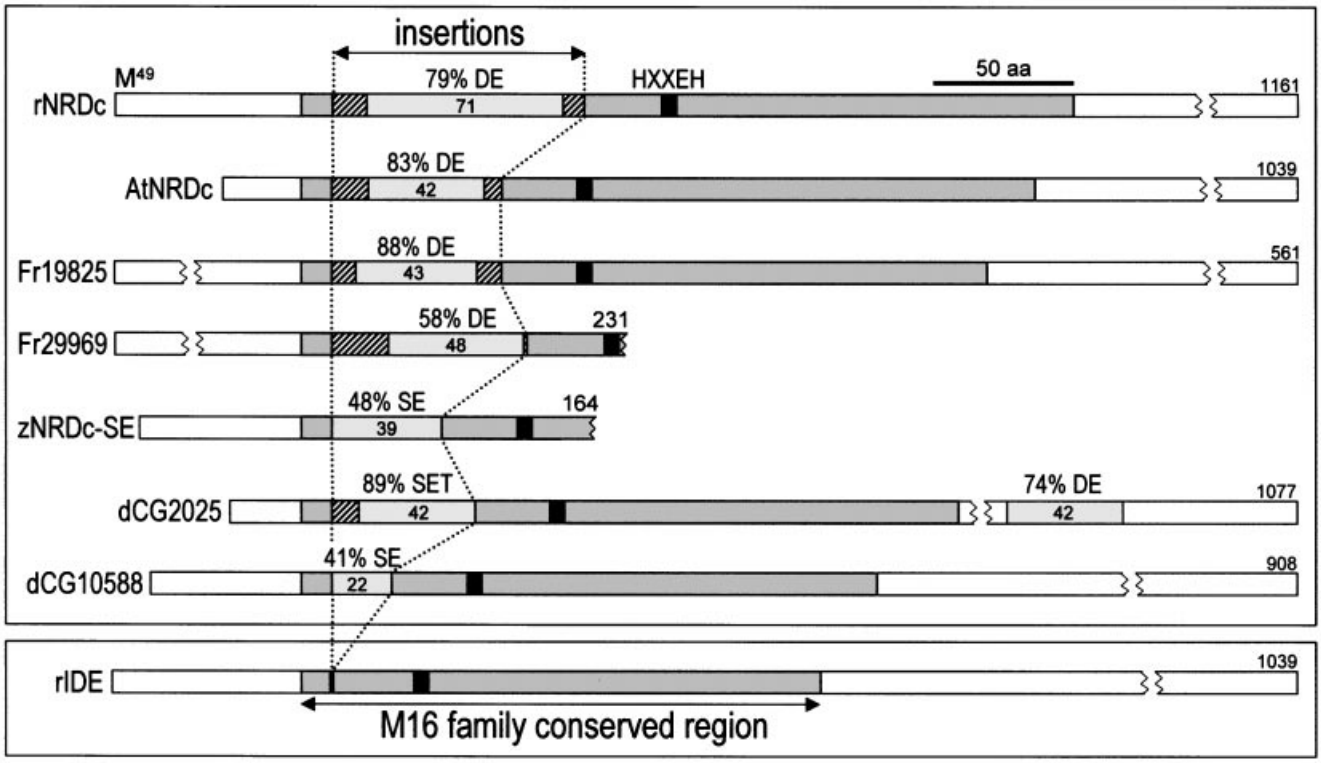

Figure 1 Schematic alignment of NRDc-like M16 family members exhibiting one or more insertions in the catalytic region

The conserved region of the M16 family (186 amino acids; dark grey box in rIDE; lower panel) comprises the HXXEH binding motif of catalytic Zn^{2+} (black box). Insertion-containing members are shown in the upper panel. Length of the acidic (DE) or Ser-Glu and Ser-Glu-Thr (SE and SET)-rich stretches (light grey boxes) and their contents (%) of Glu + Asp (DE), Ser + Glu + Asp (SE) and Ser + Glu + Asp + Thr (SET) are indicated. These stretches are either flanked or not by short sequences (hatched boxes) non-homologous to the M16 family consensus. Note that, in addition to its SET domain, dCG2025 possesses an acidic stretch located $\approx$ 50 amino acids upstream of its C-terminus. Accesssion numbers: rNRDc, NP037125; AtNRDc (*A. thaliana* putative NRDc), AAF63132; PDB code Fr19825 (*F. rubripes*), JGI19825; PDB code Fr29969 (*F. rubripes*), JGI29969; zNRDc-SE (*Danio rerio*), AW342949; PDB code dCG2025 (*D. melanogaster*), AAF48105; PDB code dCG10588 (*D. melanogaster*), AAF51661; rIDE (rat insulysin), S29509.

factor (HB-EGF) [17]. This member of the EGF family is a potent stimulator of cell proliferation and migration and is implicated in processes such as wound healing, smooth muscle cell hyperplasia or tumour growth [18]. HB-EGF, a ligand of the erbB1 and erbB4 isoforms of the EGF receptor (EGFR) [19], is synthesized as a transmembrane molecule whose ectodomain contains a 21 amino acid basic heparin-binding (HB) domain [20]. While transmembrane HB-EGF acts as a juxtacrine factor, its cell-surface shedding gives rise to a soluble, paracrine factor [21]. In addition, this surface processing constitutes a key step in EGFR transactivation [22]. In previous work [17], we showed that, while NRDc does not shed transmembrane HB-EGF, it can form a 150 kDa complex with soluble HB-EGF. Among the various EGFR ligands tested, only HB-EGF bound NRDc, and this binding potentiated HB-EGF-induced cell migration [17]. Modulated by either overexpression or knock-down with an antisense oligonucleotide, NRDc expression levels appeared to be correlated with the extent of cell migration enhancement [17]. NRDc enzymic activity is not required for this process, since an active-site mutant (NRDc-E^{247}A) is as potent as the wild-type enzyme. The physiological consequence of the cell-surface NRDc–HB-EGF complex formation is yet to be fully defined.

In the present study, we first identified the translation initiation site of NRDc. We then characterized the NRDc–HB-EGF interaction and demonstrated that binding involves the HB domain of HB-EGF and the DAC of NRDc. Finally we showed that HB-EGF is a potent inhibitor of NRDc activity *in vitro*.

EXPERIMENTAL

Cell culture

Human embryonic kidney HEK-293 cells were grown in Dulbecco's modified Eagle's medium containing 10% heat-inactivated fetal calf serum and 25 μg/ml gentamicin (all from Canadian Life Technologies, Burlington, ON, Canada) at 37 °C in 5% CO_2. MDA-MB 453 breast cancer cells were grown as described previously [17].

Plasmids

Addition of FLAG and V5 tags at the C-terminus of wild-type NRDc and NRDc-E^{247}A, respectively

Note that, in this study, the abbreviation 'NRDc' in the plasmid names refers to isoform 1 of rNRDc [9]. To introduce a 3′ FLAG tag, the NRDc sequence was PCR-amplified with a sense oligonucleotide (5′-AGAGGATGCATTCAATACTC-3′) spanning a unique *Nsi*I site (underlined), and an antisense oligonucleotide (5′-AAGC**TTA**ATTAAGCTCGAGTTTGACTAT-

CTTATGGTAGG-3′) introducing *Xho*I and *Pac*I sites (underlined) upstream of the stop codon (in bold) and a *Hin*dIII site. The PCR product was cloned into pGEM-9Zf(−) (Promega Corporation, Madison, WI, U.S.A.). A pCMV-Tag4 (Stratagene, La Jolla, CA, U.S.A.)-derived 48 bp *Xho*I–*Pac*I fragment containing the FLAG sequence was then introduced into the recombinant pGEM vector. The FLAG-containing *Nsi*I–*Hin*dIII NRDc fragment was then substituted for that of the recombinant vaccinia virus vector pMJ601-NRDc [6]. A two-step PCR was performed to introduce 42 bp encoding the 14 amino acid V5 epitope (Invitrogen, Carlsbad, CA, U.S.A.) upstream of the stop codon of NRDc-E^{247}A [17] cloned into the pMJ601 vector. First, two contiguous fragments were PCR-amplified using four oligonucleotides, with the two central ones introducing the V5 sequence and containing 30 complementary bases. The 5′ fragment (F1) was obtained with the above sense *Nsi*I oligonucleotide and a V5-NRDc antisense oligonucleotide (5′-ATCGAGACC-AAGGAGAGGGTTAGGGATAGGCTTACCTTGACTAT-CTTATGGTAGG-3′), and the 3′ fragment (F2) with a sense V5/pMJ601 oligonucleotide (5′-AACCCTCTCCTTGGTCTC-GATTCTACGT*AAGCTT*CGACAAGCTCGTAAAAGT-3′; *Hin*dIII site shown in italics) and an antisense pMJ601-specific oligonucleotide (5′-CAAATTCAGACGGCAAACGAC-3′). In a second step, a new PCR was performed with a mixture of F1 and F2 as a template and the two distal oligonucleotides (F1 sense and F2 antisense). The PCR product was directly digested with *Nsi*I and *Hin*dIII and the resulting 459 bp fragment was used to substitute that of pMJ601-NRDc-E^{247}A. After digestion of recombinant pMJ601 vectors with *Sal*I and *Hin*dIII, the full-length wild-type NRDc-FLAG or active-site mutant NRDc-E^{247}A-V5 was introduced in the antisense orientation into pcDNA3.1/Zeo (+) (Invitrogen) between the *Xho*I and *Hin*dIII sites. The recombinant vectors were then digested with *Nhe*I and *Xba*I and the NRDc inserts cloned into the *Nhe*I site of pIRES2-EGFP (Clontech, Palo Alto, CA, U.S.A.).

NRDc-ΔDAC- and NRDc-ΔDACΔORF_0-encoding plasmids

Deletion of the DAC sequence (corresponding to amino acids 127–214) was achieved by a two-step PCR (see above) using as a template, either pMJ601-NRDc (full-length NRDc and its 64-base upstream untranslated region) or pMJ601-NRDcΔORF_0 (pMJ601-rNRD1 in [6]) missing the NRDc 5′ untranslated region. The use of two oligonucleotides overlapping the DAC insertion site (5′-GGCTCTTTTGATTTCAGATAAGAAAACCACTG-AGAAAC-3′ and 5′-GTTTCTCAGTGGTTTTCTTATCTGA-AATCAAAAGAGCC-3′) and two distal oligonucleotides, a pMJ601-specific one (5′-ACATTGTTGAATTGGATCAGC-3′) and an antisense one overlapping the second *Bgl*II site of the NRDc sequence (5′-TATCTGAGTGAAGATCTCC-3′) led to 1120 or 1040 bp amplified fragments. The latter were used to generate two recombinant pENTR-2B vectors (Gateway cloning technology; Canadian Life Technologies) encoding a DAC-deleted NRDc (ΔDAC), missing (ΔORF_0) or not its 5′ untranslated region. By recombination with the pDEST12.2 vector (Gateway cloning technology), the expression vectors pEXP-NRDc-ΔDAC and pEXP-NRDc-ΔDACΔORF_0 were finally obtained.

pGEX-DAC vector

The DAC coding sequence (corresponding to amino acids 127–214) was amplified using two oligonucleotides (5′-GGAAT-TCTGAGCAATGTGGAGGGTAAAACCGG-3′ and 5′-GG-AATTCACGGGCTTCCACACGCTCTTCG-3′) and the PCR fragment was introduced at the *Eco*RI site of pGEX-KT [23] to generate pGEX-DAC.

Preparation of the fusion protein glutathione S-transferase (GST)-DAC

Escherichia coli strain BL21 (Stratagene) transformed with pGEX-DAC were grown in Luria–Bertani medium to a *D* value of ≈ 1 and the fusion protein expression was induced by addition of 0.5 mM isopropyl β-D-thiogalactoside (Sigma-Aldrich, Oakville, ON, Canada). The cells were grown for an additional 3 h, collected by centrifugation and resuspended in 60 ml of lysis buffer (20 mM Tris/HCl, pH 8, 100 mM NaCl, 1 mM EDTA, 1 mM dithiothreitol and 0.5% Nonidet P-40). After sonication and centrifugation at 4 °C for 30 min at 20000 ***g***, the supernatant was collected, adjusted to 50 mM KCl, 50 mM Tris/HCl, pH 7.5, and loaded on to a DEAE column (10 ml bead volume) pre-equilibrated with 150 mM KCl, 50 mM Tris/HCl, pH 7.5. Fractions obtained by elution with a 31 ml linear salt gradient from 150 to 600 mM KCl in 50 mM Tris/HCl, pH 7.5, were analysed, and the GST-DAC-containing fractions were pooled and further batch-purified on glutathione–Sepharose 4B (Amersham Biosciences, Baie d'Urfé, QC, Canada) as recommended by the manufacturer. The eluted proteins were then washed with PBS and concentrated in an Amicon Centriprep 10K filtration unit (Millipore Corporation, Bedford, MA, U.S.A.). GST-DAC was then used to obtain a rabbit polyclonal antiserum and kept in aliquots at −80 °C.

Radioiodination and chemical cross-linking

Cross-linking of [^{125}I]HB-EGF at the cell surface and in solution with recombinant NRDc were carried out as described previously [17]. In competition experiments, various amounts of P21 [24] and peptide 3100 unlabelled peptides were added to [^{125}I]HB-EGF. These peptides correspond to the HB domain (amino acids 93–113) and cytosolic tail (amino acids 193–208) of HB-EGF, respectively.

Transient transfections and cell-surface biotinylation

The pIRES2-EGF, pIRES-NRDc-Flag, pIRES-NRDc-E^{247}A-V5, pEXP-NRDc-ΔDAC and pEXP-NRDc-ΔDACΔORF_0 vectors were transiently transfected into HEK-293 cells using Effectene (Qiagen, Mississauga, ON, CA). Briefly, 24 h before transfection, cells were plated either on 60 mm plates (6.5×10^5 cells) for biotinylation of cell-surface proteins or 100 mm plates (1.5×10^6 cells) for enzyme preparation and were then transfected with 1.5 or 3 μg of DNA, respectively. The medium was replaced 24 h after transfection and cells were grown for an additional 24 h before being harvested or biotinylated as described previously [6].

Enzyme preparation

After three washes with PBS, transfected HEK-293 cells were resuspended in 50 mM Tris/HCl, pH 7.5, 5 mM 2-mercaptoethanol and 0.05% Triton X-100, broken by repeated passages through a 25-gauge needle and then centrifugated at 27000 ***g*** for 15 min at 4 °C. Supernatants were immunoprecipitated with antibodies directed against V5 (diluted 1/250) or FLAG epitopes (diluted 1/200). The immunoprecipitated proteins, conserved at 4 °C in 20 mM potassium phosphate, pH 7.2, containing 10% glycerol, were analysed by SDS/PAGE (8% gel) and silver staining or Western blotting, and used in enzymic assays.

Enzymic assay and determination of IC_{50} values

Assays were carried out by incubation at 37 °C for 15 min of an aliquot of the enzyme preparation with dynorphin A (12 μM; Sigma-Aldrich) in 250 mM Tris/HCl, pH 8.9, in a 100 μl final volume. These incubation conditions were found to be optimal for dynorphin A processing by NRDc [3,6]. The reaction was stopped by adding 10 μl of acetic acid and analysed by reversed-phase HPLC (C_{18} column, 80 Å, 5 μm; 3.9 mm × 300 mm; Chromatography Science Company, Montreal, QC, Canada) using a 16 min 28–60 % acetonitrile gradient in 0.1 % trifluoroacetic acid. To determine the effect of growth factors, P21, calcium and GST-DAC, a quantity of enzyme achieving 25 % cleavage in 15 min at 37 °C (giving the 100 % reference for each experiment) was preincubated with these agents for 15 min at 37 °C prior to addition of the substrate. These conditions allow the accurate measurement of the dynorphin A products within the range of 2.5–25 % digestion. IC_{50} values were determined by Grafit4 or Sigma-Plot programs.

Western blotting and antibodies

Immunoprecipitated and purified proteins were separated by SDS/PAGE on 8 % or 12 % gels and transferred to nitrocellulose filters (Hybond-ECL; Amersham Biosciences). After blocking with 5 % non-fat dry milk in TBS-T (10 mM Tris/HCl, pH 7.5, 150 mM NaCl and 0.05 % Tween-20), filters were incubated with anti-NRDc [3], anti-GST-DAC (see above), anti-V5 (Stratagene) or anti-FLAG (Invitrogen) antibodies, all at a dilution of 1:5000, except for anti-FLAG which was used at 1:1000. The antigen–antibody complexes were revealed using horseradish peroxidase-conjugated anti-rabbit (Sigma-Aldrich) or anti-mouse (Amersham Biosciences) IgGs and enhanced chemiluminescence (ECL Plus; Amersham Biosciences).

Analysis of NRDc digestion of P21, reduced P21 and P21-CS

Reduced P21 (4 mM) was obtained by incubation in 100 mM dithiothreitol at 100 °C for 3 min followed by a rapid cooling at 4 °C. P21-CS is a P21 derivative with a Cys^{16}-to-Ser substitution. Peptides (30 μM) were incubated with an aliquot of the enzyme preparation at 37 °C for 2, 10, 30 and 60 min in 250 mM Tris/HCl, pH 8.9. Digestion products were separated by reversed-phase HPLC (see above for the characteristics of the column), using a 40 min 15–55 % acetonitrile gradient in 0.1 % trifluoroacetic acid, and collected. Digestion products were identified by MS on a matrix-assisted laser-desorption ionization–time-of-flight (MALDI-TOF) Voyageur DE-Pro instrument (PE PerSeptive Biosystems, Framingham, MA, U.S.A.) using the matrix 3,5-dimethoxy-4-hydroxy-cinnamic acid (Sigma-Aldrich).

RESULTS

The DAC is dispensable for NRDc catalytic activity and cellular export

Since NRDc is characterized by its DAC inserted within the highly conserved catalytic region (Figure 1), we first sought to define its importance for NRDc activity. Accordingly, we designed an NRDc mutant missing this domain (NRDc-ΔDAC). Since the DAC is a key element in the enzyme-purification protocol, C-terminal epitopes were introduced in wild-type and mutant recombinant proteins to facilitate their recovery by immunoprecipitation (Figure 2). An active-site mutant, NRDc-E^{247}A, in which the HXXEH Zn^{2+}-binding motif was mutated to HXXAH [17], was also analysed. Wild-type NRDc and its

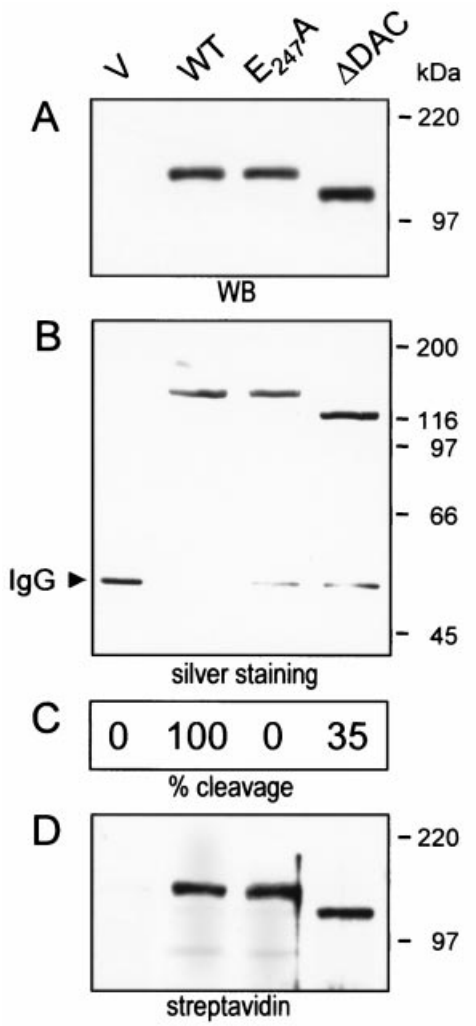

Figure 2 Expression and cellular analysis of NRDc and its mutants

(**A**) Anti-NRDc Western-blot analysis of lysates of HEK-293 cells transfected with an empty pIRES2-EGFP vector (V), or vectors expressing wild-type NRDc (WT), its active-site mutant (E^{247}A) or NRDc-ΔDAC (ΔDAC). (**B**) Silver staining analysis of recombinant NRDc immunoprecipitated with antibodies directed against a C-terminal FLAG (WT) or V5 (E^{247}A and ΔDAC). The migration position of the immunoglobulin heavy chain (IgG) is emphasized. (**C**) Normalized *in vitro* activities towards dynorphin A of immunoprecipitated NRDc (% cleavage). (**D**) Streptavidin revelation of immunoprecipitated proteins with NRDc antibodies after biotinylation of cell-surface proteins.

mutants were well expressed in transiently transfected HEK-293 cells, as illustrated by Western blotting with an NRDc antibody (Figure 2A). These recombinants were immunoprecipitated with either FLAG (wild type) or V5 (E^{247}A and ΔDAC) antibodies. Activity measurements of the purified enzymes showed that equal quantities (as assessed by silver staining) of testis and immunoprecipitated NRDc had similar activities, strongly suggesting that they share comparable specific activities. Upon normalization of protein contents (Figure 2B), the data revealed that while the active-site mutant was inactive, the DAC deletion did not abolish the activity but only reduced it by a factor of ≈ 3 (Figure 2C). Although removal of the DAC may have slightly changed the conformation of the catalytic domain, the DAC may also play a direct role in substrate binding/presentation. In any case, the 3-fold reduction in enzyme activity suggests that the

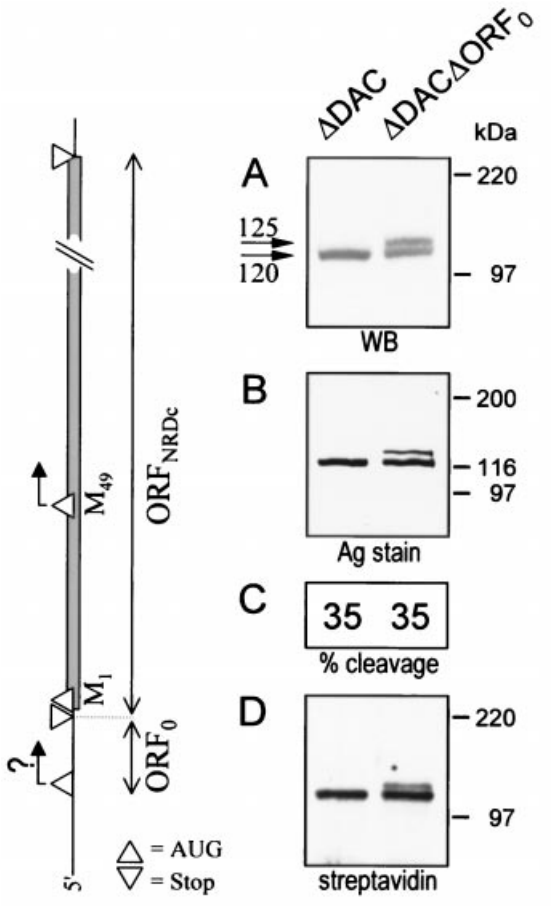

Figure 3 Initiation of NRDc translation at Met[49]

(**A**) Anti-NRDc Western-blot analysis of NRDc-ΔDAC (ΔDAC) and a derived mutant (ΔORF_0), in which the entire 5′ upstream sequence containing a small ORF was replaced by 6 nt, providing the Kozak's consensus to Met[1] AUG. (**B**) Silver staining analysis of immunoprecipitated proteins with anti-C-terminal V5. (**C**) Normalized *in vitro* activities towards dynorphin A of the immunoprecipitated NRDc (% cleavage). (**D**) Streptavidin revelation of immunoprecipitated proteins with NRDc antibodies after biotinylation of cell-surface proteins. The diagram on the left depicts the working hypothesis: translation of the short upstream ORF_0 (arrow plus question mark) hampers re-initiation at the adjacent Met_1 codon of ORF_{NRDc} and forces it to take place at the following AUG codon, i.e. at Met_{49} (arrow).

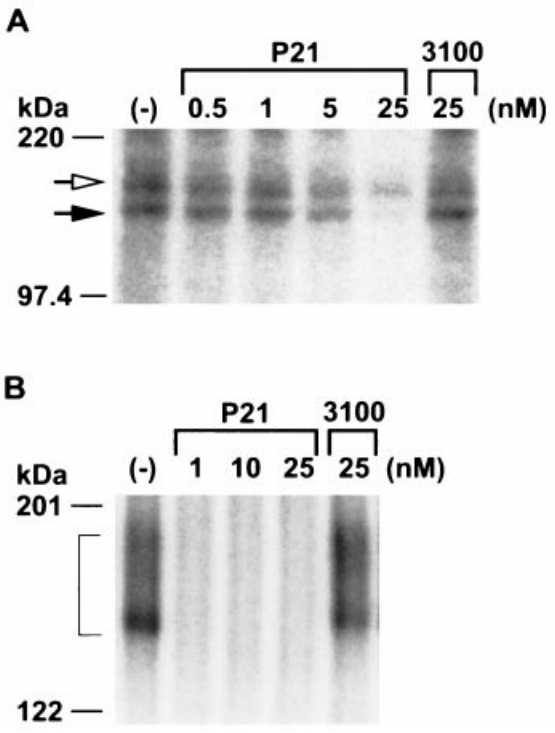

Figure 4 P21 competes for HB-EGF binding to NRDc (A) at the cell surface or (B) in solution

(**A**) ^{125}I-HB-EGF (0.5 nM) was incubated with MDA-MB 453 cells in the absence (—) or presence of P21 that mimics the HB domain of HB-EGF. After cross-linking and cell lysis, the complexes were analysed by SDS/PAGE and autoradiography. White and black arrows point at HB-EGF–erbB1 and HB-EGF–NRDc complexes, respectively. (**B**) ^{125}I-HB-EGF (3.5 nM) was cross-linked to rNRDc in solution in the absence (—) or presence of P21. The bracket denotes radiolabelled complexes containing ^{125}I-HB-EGF and NRDc. In both panels, the peptide 3100, which corresponds to the cytoplasmic tail of HB-EGF, had no effect on HB-EGF binding.

DAC is neither required for enzyme folding nor critical for NRDc activity. In addition, the DAC deletion had no impact on the selectivity of NRDc for cleavage in between the Arg doublet in dynorphin A (results not shown). Finally, biotinylation of intact cells was performed to check for a possible effect of the active-site mutation or DAC deletion on the export and/or retention of NRDc at the cell surface (Figure 2D). Although it is difficult to estimate the absolute percentage of cell-surface NRDc, it is legitimate to conclude that neither mutation affects the relative cell-surface level of the enzyme since, for equivalent amounts of total cellular NRDc estimated by Western-blot analysis, comparable intensities were obtained by streptavidin revelation.

NRDc translation initiates at Met[49]

N-terminal sequencing of immunoprecipitated NRDc and NRDc-ΔDAC revealed that both proteins start at Pro[50] (results not shown). rNRDc purified from testis or overexpressing BSC40 cells started at Val[77] and Gly[81] respectively [6]. In contrast, human or mouse NRDc purified from MDA-MB 453 cells [17] or overexpressing Sf9 cells [25], respectively, started at Pro[49] (equivalent to Pro[50] in the rat sequence). The hypothesis of Met[49] as the translation initiation site of NRDc was also based on (i) the M16 family multiple alignment (see above), (ii) the presence of a 27 nt upstream open reading frame (ORF_0) with a stop codon adjacent to the Met[1] codon [15] (the latter configuration may favour reinitiation at the second AUG (Met[49]) [26]), and (iii) the fact that initiator methionines of cytosolic proteins are usually eliminated [27], rationalizing the observed N-terminal Pro[50]. To verify this hypothesis, the 5′ upstream sequence (64 nt) containing ORF_0 was replaced by 6 nt introducing the Kozak's consensus [28] for efficient initiation at Met[1]. To show more clearly the expected 5 kDa difference in protein mass between initiation at Met[1] or Met[49], the ΔORF_0 mutation was introduced into NRDc-ΔDAC that had a smaller size (Figure 2). In addition to the $\approx$ 120 kDa product starting at Pro[50] observed in NRDc-ΔDAC-expressing cells, the ΔORF_0 mutation led to the appearance of a higher-mass product ($\approx$ 125 kDa; Figures 3A and 3B). Thus even under optimized translational conditions, initiation at Met[1] remained inefficient. The mixture of the two species exhibited an activity similar to that of the 120 kDa species alone (Figure 3C). Both forms were also exported to the cell surface with equal efficiency (Figure 3D).

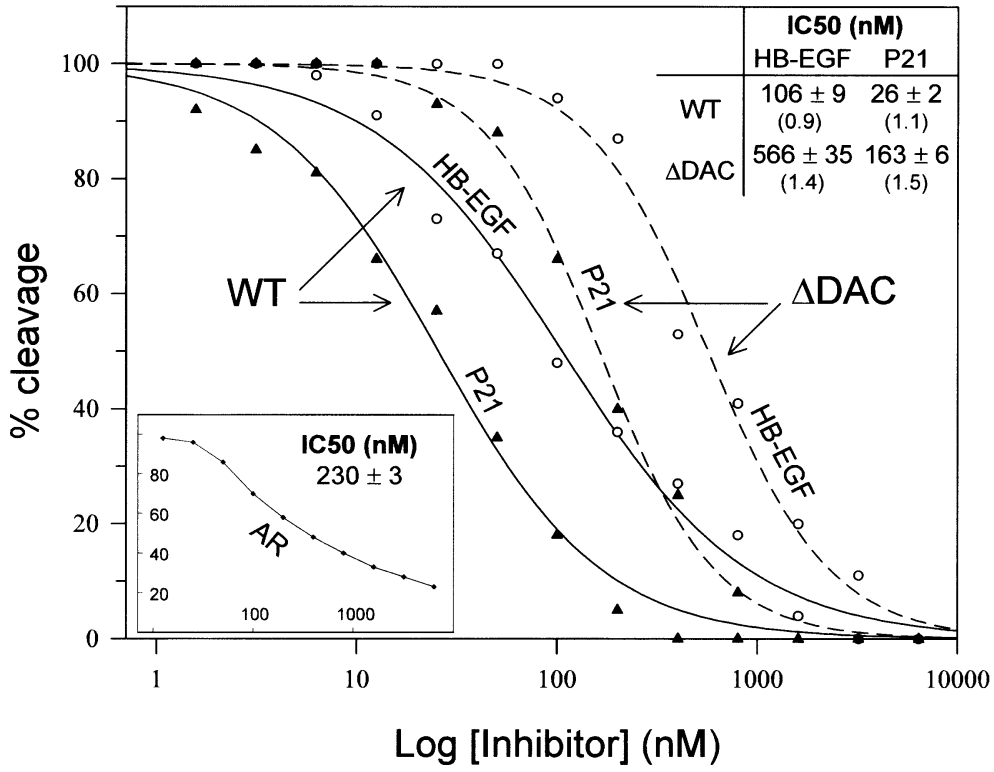

Figure 5 HB-EGF, P21 or amphiregulin inhibition of wild-type or ΔDAC-NRDc

Inhibition curves of NRDc (WT) or NRDc-ΔDAC (ΔDAC) by P21 (▲), HB-EGF (○) or amphiregulin (AR; inset). The corresponding IC_{50} and slope factors (in parentheses) are indicated. These values were obtained using the GraFit program except for amphiregulin, whose IC_{50} was determined by using the Sigma Plot program.

Table 1 NRDc cleavage products of reduced P21 and P21-CS

The peptides were incubated with NRDc for various times and the cleavage products were resolved by reversed-phase HPLC. Their retention times and mass spectral sizes are shown, as well as their calculated masses. The sites of major and minor cleavage are indicated by inverted triangles and arrows, respectively.

Reduced P21

▽↓ ↓ ▽
KRKKKGKGLGKKRDPCLRKYK
5 10 15 20

Ret. Time (min)	Observed Mass (Da)	Peptide	Calculated Mass (Da)
18	1100.12	1-10 ↓	1099.7
18	1685.33	↓ 4-18 ▽	1684.0
19	1812.64	▽ 3-18 ▽	1812.1
24	2106.00	↓ 4-21	2103.3
25	2516.52	1-21	2516.6

P21-CS

↓↓ ▽↓▽ ↓
KRKKKGKGLGKKRDP**S**LRKYK
5 10 15 20

Ret. Time (min)	Observed Mass (Da)	Peptide	Calculated Mass (Da)
19	1291.42	↓ 12-21	1290.8
19	1163.24	▽ 13-21	1162.7
20	1419.35	▽ 11-21	1418.8
23	2216.93	↓ 3-21	2215.4
23	2087.78	↓ 4-21	2087.3
25	741.65	▽ 13-18 ↓	743.4
25	2500.61	1-21	2500.7

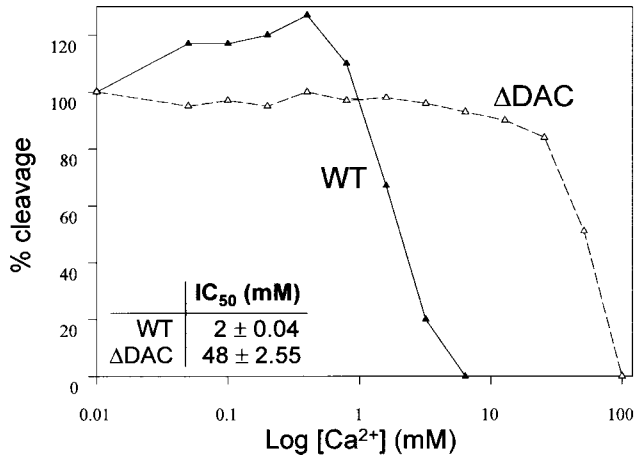

Figure 6 NRDc sensitivity to Ca^{2+} is mediated by DAC

Effect of Ca^{2+} on NRDc (WT; ▲) and NRDc-ΔDAC (ΔDAC; △) enzymic activities in 250 mM Tris/HCl, pH 8.9.

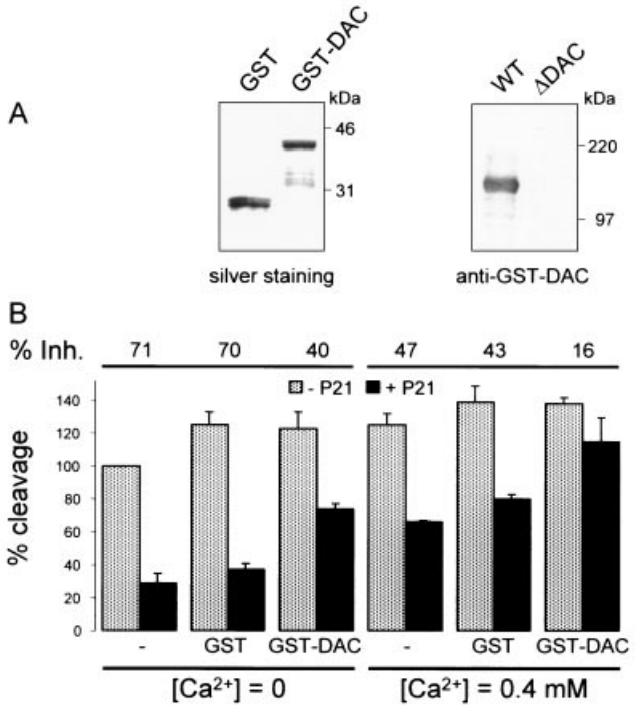

Figure 7 Analysis of the GST-DAC fusion protein and its effect on NRDc inhibition by P21 in the absence or presence of Ca^{2+}

(**A**) Purified GST or GST-DAC (≈ 600 ng each) was analysed by SDS/PAGE (12% gel) and silver staining (left-hand panel). As expected, anti-GST-DAC antibodies recognize wild-type (WT) NRDc but not NRDc-ΔDAC (ΔDAC; right-hand panel). (**B**) Effect of GST or GST-DAC on P21 inhibition of NRDc in the absence (left-hand panel) or presence (right-hand panel) of Ca^{2+}. Wild-type NRDc was preincubated for 15 min at 37 °C in the absence or presence of GST, GST-DAC or Ca^{2+}. Dynorphin A was then added and the digestion allowed to proceed for an additional 15 min. The 25% cleavage achieved in the absence of any effector was taken as the 100% value (left-most bar). [P21] = 80 nM, [GST] and [GST-DAC] = 300 nM.

The HB domain of HB-EGF binds to NRDc

We previously showed that, among other EGFR ligands tested, only amphiregulin competed with HB-EGF for NRDc binding, albeit only *in vitro* [17]. Since amphiregulin has an HB domain very similar to that of HB-EGF, the hypothesis of the involvement of this domain in NRDc binding was examined. Intact cells or NRDc in solution were incubated with iodinated HB-EGF in the absence or presence of either P21, a 21 amino acid peptide mimicking the HB domain of HB-EGF [24] or, as a negative control, peptide 3100 that corresponds to the HB-EGF cytosolic tail. After cross-linking, cells were lysed, and cell lysates (Figure 4A) or *in vitro* incubation mixtures (Figure 4B) were analysed by electrophoresis and autoradiography (Figure 4). P21 competed more efficiently with the formation of the NRDc–HB-EGF complex (150 kDa, the lower band in Figure 4A [17]) than with the erbB1–HB-EGF complex (upper band in Figure 4A). P21 also abolished HB-EGF binding to heparan sulphate proteoglycans, which appeared as a background on the gel, but only partially inhibited binding of HB-EGF to erbB1. In solution (Figure 4B), P21 efficiently displaced NRDc at concentrations $\geqslant 1$ nM instead of the 25 nM needed to achieve the same result at the cell surface (Figure 4A). In both cases, peptide 3100 had no effect. These results implicate the HB domain of HB-EGF in NRDc binding.

HB-EGF and P21 inhibit NRDc

Neither HB-EGF nor P21 behaved as substrates according to HPLC and mass spectral analyses of incubation mixtures containing high concentrations of wild-type NRDc (results not shown). On the other hand, both had strong inhibitory effects on NRDc activity with IC_{50} values of 106 and 26 nM, respectively (Figure 5). The fact that P21 is as good an inhibitor as, or even better than, HB-EGF suggests that the HB domain is the sole determinant involved in NRDc inhibition. Since the HB domain contains 12 positively charged residues (see sequence in Table 1) and several potential cleavage sites for NRDc, we hypothesized that it inhibited NRDc either directly through binding to the active site or indirectly via interaction with the negatively charged DAC.

The DAC contributes to HB-EGF binding

As shown in Figure 5, the DAC deletion did not prevent HB-EGF or P21 inhibition, but led to a 6-fold lower sensitivity (see IC_{50} inset) and to steeper slopes of inhibition curves. Therefore, although not solely involved, the DAC may be an important element in HB domain interaction. As expected from previous *ex vivo* experiments that suggested a much lower affinity for NRDc [17], amphiregulin is a rather inefficient inhibitor (Figure 5, inset).

Because acidic stretches usually show high capacity and low affinity for Ca^{2+} ($K_d \approx 10^{-3}$ M) [29], we investigated whether Ca^{2+} could regulate NRDc activity (Figure 6). At concentrations > 1 mM, Ca^{2+} inhibited NRDc ($IC_{50} = 2$ mM). Since NRDc-ΔDAC was ≈ 25-fold less sensitive than NRDc ($IC_{50} = 48$ mM), we deduce that Ca^{2+} inhibition is mainly mediated through the DAC. Note that a slight activation (≈ 20%) was observed at lower Ca^{2+} concentrations, peaking at 0.4 mM.

To probe the existence of a direct interaction between the DAC and HB-EGF, we used a fusion protein in which GST was fused to the N-terminal of the 90 amino acid DAC (GST-DAC). The protein was purified (Figure 7A, left-hand panel) and the final preparation injected into rabbits, generating antibodies that recognized the wild-type enzyme but not NRDc-ΔDAC (Figure 7A, right-hand panel). In the absence of Ca^{2+} (Figure 7B), while GST did not affect the inhibitory potency of P21 (71 compared

with 70% inhibition), GST-DAC reduced it by a factor of ≈ 2 (71 compared with 40% inhibition). The presence of Ca^{2+} (0.4 mM; Figure 7B) led to a 34% lower inhibitory potency of P21 (71 versus 47% inhibition). Under these Ca^{2+} conditions, GST also did not affect P21 inhibition (47 versus 43% inhibition) whereas GST-DAC reduced it by a factor ≈ 3 (47 versus 16% inhibition). We can thus conclude that (i) through binding to the DAC, Ca^{2+} in the higher μM range activates NRDc and attenuates its inhibition by the HB domain and (ii) GST-DAC can compete with NRDc for P21 binding, indicating that the DAC directly binds the HB domain. In agreement, GST-DAC abrogates the HB-EGF inhibition of NRDc processing of dynorphin A (results not shown).

Disulphide-bonded P21 is the NRDc inhibitor

Whereas P21 is a potent inhibitor of NRDc, it has less effect on NRDc-ΔDAC (Figure 5). This suggested that the latter may partially cleave P21. Indeed, reversed-phase HPLC and MS analysis of P21 digestion products confirmed that P21 is not processed by NRDc but partially cleaved by NRDc-ΔDAC at $Arg\downarrow Lys^{3}$ and $Arg\downarrow Lys^{19}$, generating the peptide 3-18 (results not shown). Thus, P21 enters the catalytic pocket of NRDc-ΔDAC. Whether P21 also interacts with the pocket of NRDc, though more efficiently since it is a strong inhibitor, or inhibits NRDc via its binding to a distinct site is not yet clear. In addition, MS analysis of P21 revealed a mixture of monomers and dimers (results not shown), most probably due to the presence of a single Cys residue. Indeed, in HB-EGF, the HB domain slightly overlaps the EGF-like sequence and, as a result, comprises the first (position 16) of the six cysteines. Since monomers and dimers may inhibit NRDc differently, we tested the inhibitory effect of reduced P21 and P21-CS, a P21 derivative in which Cys^{16} was substituted by Ser. Reduced P21 was cleaved at the same sites by NRDc as native P21 was by NRDc-ΔDAC. In addition, two minor sites were also identified (Table 1). Curiously, P21-CS was cleaved differently than reduced P21, with the two major sites occurring at $Gly\downarrow Lys^{11}Lys\downarrow Arg^{13}$. Thus, reduced Cys in P21 cannot be replaced by Ser without affecting P21 susceptibility to NRDc. We conclude that in the P21 mixture the disulphide bonded P21 is most likely the inhibitory species and that reduced P21 and P21-CS are not inhibitors but behave as substrates that directly bind to the active site of NRDc.

DISCUSSION

NRDc is a metalloendopeptidase that belongs to the M16 family (Figure 1) and cleaves peptides at basic sites *in vitro* [4,15]. Although cytosolic, it is also exported to the surface of several cell types [6,17]. However, its cytosolic and/or extracellular substrate(s) remain to be identified. The recent discovery that NRDc binds HB-EGF at the cell surface and enhances the induced cellular migration gave a first insight into one of its physiological properties [17]. Since neither HB-EGF binding nor enhancement of the HB-EGF-induced migration necessitates NRDc enzymic activity [17], this suggests that the protein fulfills a second function as an HB-EGF modulator. This is reminiscent of other metalloendopeptidases that exhibit dual functions, like the two M16 family members yeast Axl1 protein and mitochondrial processing peptidase (MPP). Aside from its involvement in the N-terminal processing of the a-factor [30], Axl1 is an essential morphogenic determinant in yeast budding (axial/bipolar) [31]. In some organisms, MPP that removes mitochondrial targeting sequences from nuclear-encoded proteins also acts as a core subunit of cytochrome *c* reductase, a protein complex of the respiratory chain [32]. Similarly, the metallopeptidase carboxypeptidase E that trims basic residues [33] is also implicated in protein sorting to secretory granules [34].

In the present and previous studies [6,17,25] none of the identified N-termini of NRDc were located upstream of Pro^{50}. We showed here that the first 49 residues do not constitute a rapidly processed proregion but are rather not translated. The removal of a small upstream ORF and optimization of the Met^{1} AUG context led to the appearance of a higher-mass product, suggesting that, *in vivo*, translation only initiates at Met^{49} (Figure 3). In agreement, Ma et al. [25] failed to detect, even in the presence of high concentrations of protease inhibitors, a hexa-His-tagged NRDc downstream of Met^{1}.

A distinct feature of NRDc resides in its 90 amino acid acidic domain (DAC), inserted in the conserved catalytic region, only 30 residues upstream of the HXXEH catalytic site (Figure 1). Whereas no NRDc-like sequences containing an insertion were detected in the completed genomes of *Saccharomyces cerevisiae* and *Caenorhabditis elegans*, so far one NRDc has been identified in mammals, *A. thaliana* and zebrafish and two in *Fugu* and *Drosophila* (Figure 1). The conservation of these insertions through evolution and their sequence divergence may reflect a specialization of this subfamily of proteins towards specific substrates and/or ligands. In NRDc, the acidic insertion is dispensable for catalytic activity (Figure 2), suggesting that it is not required for enzyme folding. Rather, the DAC seems to constitute an appendix to the global enzyme structure that regulates NRDc functions: (i) it seems to behave as a *cis*-activator, increasing either catalytic efficiency or enzyme stability since its removal led to a 3-fold decrease of NRDc activity; (ii) it largely contributes to HB-EGF binding by interacting with the HB domain (Figures 4 and 5); and (iii) through Ca^{2+} binding, it regulates both NRDc enzymic activity (Figure 6) and its interaction with HB-EGF (Figures 5 and 7). Thus, *in vivo*, extracellular Ca^{2+} (basal levels, 1–2 mM) that increases under hypercalcimic or secretory conditions may regulate the physiological functions of NRDc. In contrast, in the cytoplasm, NRDc would be insensitive to the lower Ca^{2+} concentrations (50–100 μM).

We showed that, *in vitro*, HB-EGF is not a substrate but a potent inhibitor of the enzyme (Figure 5). Evidence that its HB domain is involved in NRDc binding came from the competing effect of P21 on HB-EGF binding to NRDc at the cell surface and *in vitro* (Figure 4). In addition, the P21 higher inhibitory effect (IC_{50} = 26 nM) versus that of HB-EGF (IC_{50} = 100 nM; Figure 5) suggests that the HB domain is the sole element required for NRDc binding or inhibition. On the NRDc side, the DAC and possibly the active site seem to participate in P21 binding. The importance of the DAC is illustrated by a 6-fold drop in NRDc-ΔDAC sensitivity to HB-EGF or P21 compared with that of NRDc (Figure 5). Furthermore, preincubation of P21 with a GST-DAC fusion protein abolished its inhibitory effect, thereby indicating that the DAC can directly bind P21 (Figure 7). The remaining sensitivity of NRDc-ΔDAC to HB-EGF and P21 (Figure 5) revealed the involvement of another domain, likely to be the catalytic one. These conclusions agree with the previously reported existence of two classes of HB-EGF binding sites on NRDc [17]. The hypothesis of the participation of the active site in HB-EGF binding is reinforced by the ability of NRDc to cleave both reduced P21 and its $C^{16}S$ variant (Table 1). Whether the DAC and the active site bind one or more HB-EGF molecules, and constitute distinct high- and low-affinity binding sites, is not yet clear. Alternatively, the DAC that is located in the vicinity of the catalytic site may intervene in substrate/inhibitor selection and/or positioning. It was recently

shown that the DAC binds several spermine molecules in a co-operative manner and that the induced conformational change in NRDc could affect the active-site structure since spermine acts as a non-competitive inhibitor [25].

Analysis of the processing of reduced P21 and P21-CS confirmed the strict specificity of NRDc for cleavage upstream of basic residues in dibasic stretches. Although NRDc was reported to prefer cleavage upstream of Arg residues [3,4], all the observed P21 cleavages occurred upstream of Lys except for one of the two major cleavage sites Lys-Lys ↓ Arg^{13}Asp in P21-CS. Since kinetic analysis of reduced P21 revealed that both major cleavages occurred simultaneously (results not shown), it is not yet clear if one or both of the two sites are involved in NRDc inhibition by HB-EGF. The sole involvement of the first one is however unlikely, since HB-EGF and amphiregulin, which is a poor inhibitor, exhibit an identical Lys-Arg-Lys-Lys-Gly^{6} sequence. The proximity of the disulphide-bonded Cys to the C-terminal site may be critical in this selection. Interestingly, NRDc cleaves reduced P21 and P21-CS within the three clusters of basic residues that were shown to be important for HB-EGF interaction with heparin [35,36]. It has been proposed that heparin-binding fibroblast growth factor has to form a ternary complex with cell-surface heparan sulphate proteoglycans and its receptor for activity [37]. By analogy, NRDc may act as an HB-EGF-specific heparin-like molecule to enhance HB-EGF-induced responses. This regulation may be particularly relevant, especially in heart, a rich source of NRDc, and where HB-EGF was shown to mediate cardiac hypertrophy [38]. NRDc expression during embryogenesis is essentially restricted to neuronal cells and may thus play a role in cell migration at this stage, probably through HB-EGF binding. Although widely distributed in the adult, NRDc is not ubiquitous. In testis, for example, it is only detected in germ cells. In addition, not all cell lines tested exported NRDc to the cell surface. Although NRDc export and cell-surface retention will be the object of future studies, our data revealed that they are independent of NRDc enzymic activity and do not require the DAC (Figure 2). Finally, while NRDc may represent a new regulator of HB-EGF functions, identification of its cytosolic role is of great interest.

We are very grateful to Catherine Joulie, Ann Chamberland and Andrew Chen for their enthusiasm and excellent technical support. We also thank Valérie Chesneau and Tim Reudelhuber for their critical reading of the manuscript. This work was supported by a Canadian Institutes of Health Research group grant no. MGC-11474.

REFERENCES

1 Gluschankof, P., Morel, A., Gomez, S., Nicolas, P., Fahy, C. and Cohen, P. (1984) Enzymes processing somatostatin precursors: an Arg-Lys esteropeptidase from the rat brain cortex converting somatostatin-28 into somatostatin-14. Proc. Natl. Acad. Sci. U.S.A. **81**, 6662–6666

2 Gluschankof, P., Gomez, S., Morel, A. and Cohen, P. (1987) Enzymes that process somatostatin precursors. A novel endoprotease that cleaves before the arginine-lysine doublet is involved in somatostatin-28 convertase activity of rat brain cortex. J. Biol. Chem. **262**, 9615–9620

3 Chesneau, V., Pierotti, A. R., Barre, N., Creminon, C., Tougard, C. and Cohen, P. (1994) Isolation and characterization of a dibasic selective metalloendopeptidase from rat testes that cleaves at the amino terminus of arginine residues. J. Biol. Chem. **269**, 2056–2061

4 Chow, K. M., Csuhai, E., Juliano, M. A., St Pyrek, J., Juliano, L. and Hersh, L. B. (2000) Studies on the subsite specificity of rat nardilysin (N-arginine dibasic convertase). J. Biol. Chem. **275**, 19545–19551

5 Chesneau, V., Prat, A., Segretain, D., Hospital, V., Dupaix, A., Foulon, T., Jegou, B. and Cohen, P. (1996) NRD convertase: a putative processing endoprotease associated with the axoneme and the manchette in late spermatids. J. Cell Sci. **109**, 2737–2745

6 Hospital, V., Chesneau, V., Balogh, A., Joulie, C., Seidah, N. G., Cohen, P. and Prat, A. (2000) N-arginine dibasic convertase (nardilysin) isoforms are soluble dibasic-specific metalloendopeptidases that localize in the cytoplasm and at the cell surface. Biochem. J. **349**, 587–597

7 Fumagalli, P., Accarino, M., Egeo, A., Scartezzini, P., Rappazzo, G., Pizzuti, A., Avvantaggiato, V., Simeone, A., Arrigo, G., Zuffardi, O. et al. (1998) Human NRD convertase: a highly conserved metalloendopeptidase expressed at specific sites during development and in adult tissues. Genomics **47**, 238–245

8 Winter, A. G. and Pierotti, A. R. (2000) Gene expression of the dibasic-pair cleaving enzyme NRD convertase (N-arginine dibasic convertase) is differentially regulated in the GH3 pituitary and mat-Lu prostate cell lines. Biochem. J. **351**, 755–764

9 Hospital, V., Prat, A., Joulie, C., Cherif, D., Day, R. and Cohen, P (1997) Human and rat testis express two mRNA species encoding variants of NRD convertase, a metalloendopeptidase of the insulinase family. Biochem. J. **327**, 773–779

10 Csuhai, E., Safavi, A. and Hersh, L. B. (1995) Purification and characterization of a secreted arginine-specific dibasic cleaving enzyme from EL-4 cells. Biochemistry **34**, 12411–12419

11 Hooper, N. M. (1994) Families of zinc metalloproteases. FEBS Lett. **354**, 1–6

12 Barrett, A. J. (1998) Introduction: clan ME containing pitrilysin and its relatives. In Handbook of Proteolytic Enzymes (Barrett, A. J., Rawlings, N. D. and Woessner, J. F., eds.), pp. 1360–1379, Academic Press, London

13 Affholter, J. A., Fried, V. A. and Roth, R. A. (1988) Human insulin-degrading enzyme shares structural and functional homologies with *E. coli* protease III. Science **242**, 1415–1418

14 Baumeister, H., Muller, D., Rehbein, M. and Richter, D. (1993) The rat insulin-degrading enzyme. Molecular cloning and characterization of tissue-specific transcripts. FEBS Lett. **317**, 250–254

15 Pierotti, A. R., Prat, A., Chesneau, V., Gaudoux, F., Leseney, A. M., Foulon, T. and Cohen, P. (1994) N-arginine dibasic convertase, a metalloendopeptidase as a prototype of a class of processing enzymes. Proc. Natl. Acad. Sci. U.S.A. **91**, 6078–6082

16 Csuhai, E., Chen, G. and Hersh, L. B. (1998) Regulation of N-arginine dibasic convertase activity by amines: putative role of a novel acidic domain as an amine binding site. Biochemistry **37**, 3787–3794

17 Nishi, E., Prat, A., Hospital, V., Elenius, K. and Klagsbrun, M. (2001) N-arginine dibasic convertase is a specific receptor for heparin-binding EGF-like growth factor that mediates cell migration. EMBO J. **20**, 3342–3350

18 Raab, G. and Klagsbrun, M. (1997) Heparin-binding EGF-like growth factor. Biochim. Biophys. Acta **1333**, F179–F199

19 Elenius, K., Paul, S., Allison, G., Sun, J. and Klagsbrun, M. (1997) Activation of HER4 by heparin-binding EGF-like growth factor stimulates chemotaxis but not proliferation. EMBO J. **16**, 1268–1278

20 Higashiyama, S., Abraham, J. A., Miller, J., Fiddes, J. C. and Klagsbrun, M. (1991) A heparin-binding growth factor secreted by macrophage-like cells that is related to EGF. Science **251**, 936–939

21 Goishi, K., Higashiyama, S., Klagsbrun, M., Nakano, N., Umata, T., Ishikawa, M., Mekada, E. and Taniguchi, N. (1995) Phorbol ester induces the rapid processing of cell surface heparin-binding EGF-like growth factor: conversion from juxtacrine to paracrine growth factor activity. Mol. Biol. Cell **6**, 967–980

22 Prenzel, N., Zwick, E., Daub, H., Leserer, M., Abraham, R., Wallasch, C. and Ullrich, A. (1999) EGF receptor transactivation by G-protein-coupled receptors requires metalloproteinase cleavage of proHB-EGF. Nature (London) **402**, 884–888

23 Hakes, D. J. and Dixon, J. E. (1992) New vectors for high level expression of recombinant proteins in bacteria. Anal. Biochem. **202**, 293–298

24 Higashiyama, S., Abraham, J. A. and Klagsbrun, M. (1993) Heparin-binding EGF-like growth factor stimulation of smooth muscle cell migration: dependence on interactions with cell surface heparan sulfate. J. Cell Biol. **122**, 933–940

25 Ma, Z., Csuhai, E., Chow, K. M. and Hersh, L. B. (2001) Expression of the acidic stretch of nardilysin as a functional binding domain. Biochemistry **40**, 9447–9452

26 Kozak, M. (1999) Initiation of translation in prokaryotes and eukaryotes. Gene **234**, 187–208

27 Giglione, C., Serero, A., Pierre, M., Boisson, B. and Meinnel, T. (2000) Identification of eukaryotic peptide deformylases reveals universality of N-terminal protein processing mechanisms. EMBO J. **19**, 5916–5929

28 Kozak, M. (1987) An analysis of 5′-noncoding sequences from 699 vertebrate messenger RNAs. Nucleic Acids Res. **15**, 8125–8148

29 Baksh, S. and Michalak, M. (1991) Expression of calreticulin in *Escherichia coli* and identification of its Ca^{2+} binding domains. J. Biol. Chem. **266**, 21458–21465

30 Adames, N., Blundell, K., Ashby, M. N. and Boone, C. (1995) Role of yeast insulin-degrading enzyme homologs in propheromone processing and bud site selection. Science **270**, 464–467

31 Fujita, A., Oka, C., Arikawa, Y., Katagai, T., Tonouchi, A., Kuhara, S. and Misumi, Y. (1994) A yeast gene necessary for bud-site selection encodes a protein similar to insulin-degrading enzymes. Nature (London) **372**, 567–570

32 Braun, H. P. and Schmitz, U. K. (1995) Are the 'core' proteins of the mitochondrial bc1 complex evolutionary relics of a processing protease? Trends Biochem. Sci. **20**, 171–175
33 Fricker, L. D. (1988) Carboxypeptidase E. Annu. Rev. Physiol. **50**, 309–321
34 Cool, D. R., Normant, E., Shen, F., Chen, H. C., Pannell, L., Zhang, Y. and Loh, Y. P. (1997) Carboxypeptidase E is a regulated secretory pathway sorting receptor: genetic obliteration leads to endocrine disorders in Cpe(fat) mice. Cell **88**, 73–83
35 Besner, G. E., Whelton, D., Crissman-Combs, M. A., Steffen, C. L., Kim, G. Y. and Brigstock, D. R. (1992) Interaction of heparin-binding EGF-like growth factor (HB-EGF) with the epidermal growth factor receptor: modulation by heparin, heparinase, or synthetic heparin-binding HB-EGF fragments. Growth Factors **7**, 289–296
36 Thompson, S. A., Higashiyama, S., Wood, K., Pollitt, N. S., Damm, D., McEnroe, G., Garrick, B., Ashton, N., Lau, K., Hancock, N. et al. (1994) Characterization of sequences within heparin-binding EGF-like growth factor that mediate interaction with heparin. J. Biol. Chem. **269**, 2541–2549
37 Kan, M., Wang, F., Xu, J., Crabb, J. W., Hou, J. and McKeehan, W. L. (1993) An essential heparin-binding domain in the fibroblast growth factor receptor kinase. Science **259**, 1918–1921
38 Asakura, M., Kitakaze, M., Takashima, S., Liao, Y., Ishikura, F., Yoshinaka, T., Ohmoto, H., Node, K., Yoshino, K., Ishiguro, H. et al. (2002) Cardiac hypertrophy is inhibited by antagonism of ADAM12 processing of HB-EGF: metalloproteinase inhibitors as a new therapy. Nat. Med. **8**, 35–40

Received 23 May 2002/27 June 2002; accepted 3 July 2002
Published as BJ Immediate Publication 3 July 2002, DOI 10.1042/BJ20020822